Journal of the Optical Society of Korea, Vol. 10, No. 4, December 2006, pp. 145-156

Optics of Refractometers for Refractive Power Measurement of the Human Eye

Dong-Seob Ko*

Department of Techno-Marketing, Mokwon University, Daejeon 302-729, Korea

Byeong Ha Lee

Department of Information and Communications, Gwangju Institute of Science and Technology, Gwangju 500-712, Korea

(Received December 7, 2006 : revised December 19, 2006)

In the field of ophthalmology, many diagnostic instruments based on optical technology have been developed, such as refractometer, keratometer, corneal mapper, tonometer, fundus camera, slit lamp, laser scan ophthalmoscope and optical coherence tomography. Among them, the refractometer that is used for measuring the refractive power of the human eye has the long research history and various types have been developed. However the efforts to realize more accurate and precise measurement are still in progress. The wavefront analyzer commercialized in recent years is an excellent outcome of such efforts. In this paper, a brief account of the developmental history of various refractometers including the wavefront analyzer is summarized, and the underlying measurement principle is introduced in the view of optics. Finally, the technical issues that should be solved for getting better performance are discussed.

OCIS codes : 010.7350, 120.3890, 330.1070, 330.4460

I. INTRODUCTION

Ametropia can be described as the optical condition of the eye where the focal length of the eye lens and the eye length do not correspond each other. The discrepancy is described as the refractive power of the eye. There are two methods that enable to assess the refractive power; one is subjective and the other is objective. The subjective method relies on the response or reaction of a patient. Usually, the patient is asked to see a test chart and say what he or she sees. The objective method does not depend on the response of the patient but an instrument such as a refractometer measures without asking the patient.

A refractometer including various ophthalmic instruments [1-2] is composed of various parts such as optical system, calculating machine, display panel and electronics. Among them, the optical system mainly determines the performance of the instrument.

Study on the measuring method of refractive power has a long history [3-18]. About 400 years ago, Scheiner observed the refractive error of an eye with a so-called Scheiner disk [4]. As shown in Fig. 1, if someone with an imperfect eye views a distant light source such as a star through a disk which has two pinholes, then two images would be formed on his retina. This Scheiner disk has given the basic principle for measuring the refractive error of an eye and stands as the first optometer.

In the nineteenth century, the studies in the field of ophthalmology have been extensively carried out [5]. Helmholtz reported the empirical theories on spatial vision, color vision, motion perception and accommodation. He also invented the ophthalmoscope in

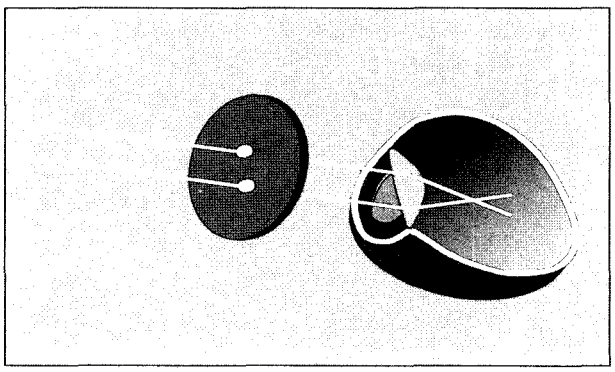

FIG. 1. Scheiner disk with the two pinholes. An ametropic eye will form two retinal images when viewing a single distant point of light such as a star through the disk.

1851 [5]. Donders was also one of the founders of the science of ophthalmology in the nineteenth century. He studied the anomalies of refraction and accommodation of the eye including farsightedness and astigmatism [5]. In 1894, Tscherning published a method to determine optical aberrations in human eyes by using an optical lens of about +5 D (diopter) which had a grid on its surface [6]. Clinical application of Tscherning's principle in ophthalmology was first introduced by Howland in 1976 [7-8].

In 1936, Reason developed a sight-testing apparatus which was able to measure the refractive power in any meridian of an eye using a rotating dove prism [9]. An ocular refractometer using an infrared light source was designed by Collins in 1937 [10]. While most of the refractometers are based on amplitude detection of light, an automatic optometer based on phase detection was proposed by Roth in 1965 [11].

In 1994, Liang reported the clinical testing of a wavefront analyzer [12]. Various wavefront analyzers (or aberrometers) for measuring the optical aberrations of eyes were developed in recent years [13-18] and widely adapted as the basic instrument that enhanced the precision of corneal ablation (or refractive surgery) [2]. The wavefront analyzer should be the most accurate refractometer for the present.

II. OPTICAL SYSTEM OF EYE REFRACTOMETER

When a collimated paraxial light beam is not focused well on the fundus of an eye, the eye is said to have refractive error or sphere error. When the actual focal point of the eye is located in front of the fundus, the eye is said to have myopia (nearsightedness). When it is located behind the fundus, it is said to have hyperopia (farsightedness). In addition to sphere error, astigmatism causes another refractive error referred to as cylinder error. The results in both cases weaken the visual acuity of the eye [19,20]. In most cases, the sphere and the cylinder error are well corrected with spectacle lenses to achieve the ideal situation of emmetropia (normal eye). However, to get the ideal correction, accurate measurement should be done ahead.

A great many methods have been made to measure the refractive power of a human eye; however, most of them are still in the research stages. In this section, the measuring principles and the characteristics of the commercialized refractometers are presented. The refractometers are categorized into three groups in view of the optics; retinoscope, autorefractor, and wavefront analyzer.

1. Retinoscope

Retinoscope (or sometimes called as skiaskope) is one of the most classical instruments that can measure the refractive power of a human eye. The retinoscope is operated manually in the objective mode [21]. The composition of the retinoscope is very simple. It is composed of a sheet-shape light source and a semi-transparent mirror as shown in Fig. 2 [1]. A light source is forced to pass a slit to form a sheet-shape light (the 'test light' in Fig. 2) and then launched into the eye of the patient by using a semi-transparent mirror. After sending the test light onto the retina of a patient, by seeing the shape and movement of the light which is reflected from the retina, the refractive power is tested.

At first, a patient and an examiner are seated face to face. The patient is asked to watch a target at infinity (generally 5 m or 6 m) and the examiner sees the eye of the patient. Then, the retina of the examiner has its conjugate image on the pupil of the patient due to the eye of the examiner. In the same way, due to the eye lens of the patient, the pupil of the examiner has its conjugate image at a place in patient's eyeball.

A part of the test light is reflected at the surface of the eye, but the part of the test light impinging into the pupil goes into the eyeball and the retina reflects it. Therefore the examiner observes two lights at the same time; the one that is reflected by the eyeball surface and the other one that is reflected by the retina of the patient. The later light has the information of the refractive power of the patient's eye. By tilting the semi-transparent mirror, the reflected point on the retina of the patient is scanned. Then, the correlation between the two lights reflected from the patient's eye

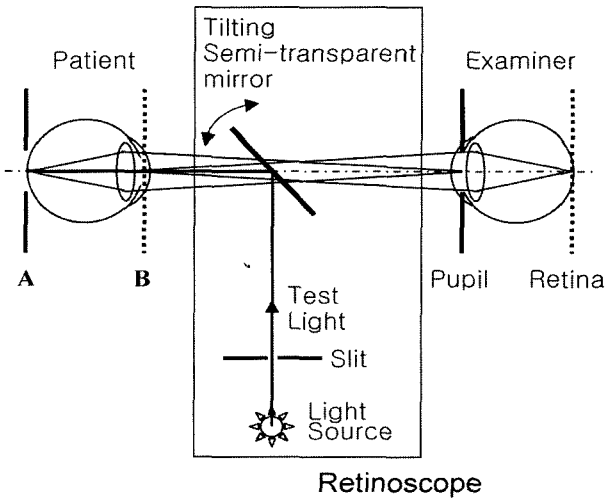

FIG. 2. A schematic diagram of a retinoscope. The lines, (A) and (B), on the patient's eye indicate the conjugate images of examiner's pupil and retina, respectively.

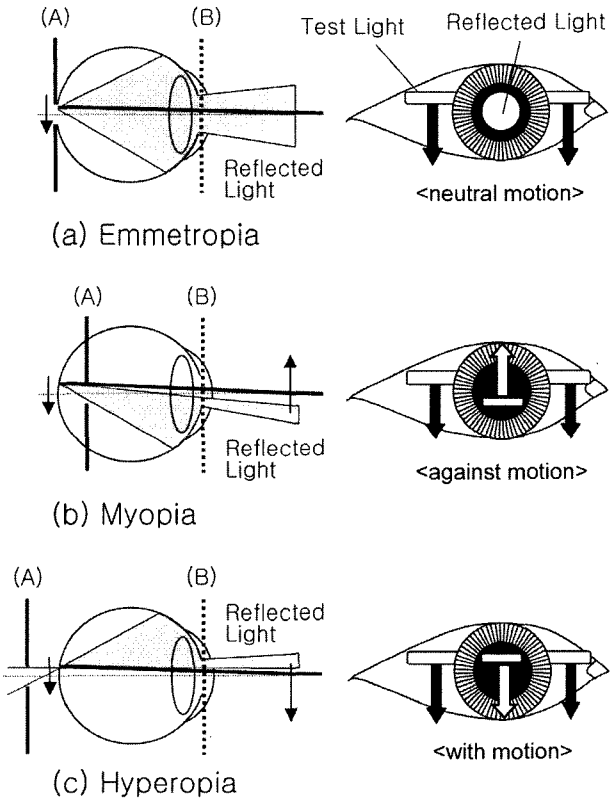

FIG. 3. Correlation between the test light and the light which is reflected from a patient's retina. The lines, (A) and (B), on the eye indicate the conjugate images of examiner's pupil and retina, respectively.

is directly related to the refractive power.

Fig. 3(a) shows the case of an emmetropia. Since the conjugate image of the examiner's pupil is located just on the retina of the patient, all the beams reflected at any point of the retina can reach the retina of the examiner. Thus, the whole part of the pupil of the patient is shining brightly. This phenomenon is called 'neutral motion' or 'complete flashing'. The important thing is that even with the tilting of the semi-transparent mirror shown in Fig. 2, thus scanning the eyeball, the flashing is not affected. It indicates emmetropia.

However, for the case of myopia, the conjugate image of the examiner's retina is located on the pupil of the patient but the conjugate image of the examiner's pupil is located in front of the retina as shown in Fig. 3(b). Therefore, the light reflected at the upper part of the patient's retina is imaged on the lower part of the conjugated examiner's retina. It means that when the test light is moved up-and-down across the pupil of the patient, the light reflected at the patient's retina moves reversely against the test light. This phenomenon is called 'against motion' and indicates myopia.

The similar thing happens with the hyperopia. As

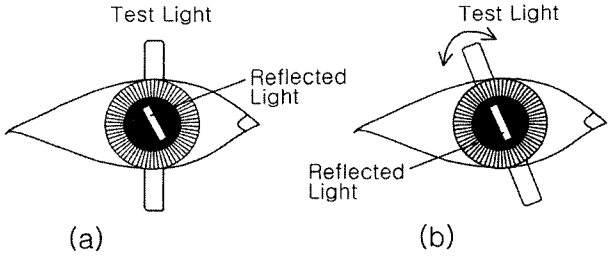

FIG. 4. For the astigmatism, the astigmatic axis can be found by rotating the test light around the pupil of the patient.

shown in Fig. 3(c), however, since the conjugate pupil image of the examiner is located back of the patient's retina, the motion is reversed. The motion of the light reflected at the retina becomes to be in the same direction with the motion of the test light. This motion is called 'with motion' and indicates hyperopia.

With this test it is possible to identify myopia and hyperopia from emmetropia. However it does not give the amount of the refractive power of the patient. To get the refractive power, a correction lens is placed in front of the patient's eye and the refractive power of the test lens or lens assembly is adjusted till the examiner observes the 'neutral motion' with the retinoscope. Then the refractive power of the lens becomes the refractive power of the patient's eye.

For the astigmatism, the test light and the reflected light are not well aligned angularly, in general, as shown in Fig. 4(a). It is called 'break phenomenon' [21]. However, by rotating the test light around the pupil of the patient, we can orient both beams along the same orientations as shown in Fig. 4(b). This orientation angle is the astigmatic axis or the one normal to it.

The measurement principle of the retinoscope that has been described above is valid only when the patient and the examiner are far apart so that emmetropic eye can have the conjugate image of the examiner's pupil on its retina. In practical cases, the measurement is made within a short distance, about 50 cm or 66 cm apart [21]. In this case the conjugate pupil image is located back of the retina of an emmetropia. The 'neutral motion' happens with a myopia. Therefore a correction of the refractive power is needed. The correction is -1.5 D for a 66 cm working distance and -2.0 D for a 50 cm working distance.

2. Autorefractor

The retinoscopy described above can measure the refractive power with an accuracy of ± 0.25 D. However the accuracy depends highly on the measurement skill of the examiner. Further, to get the amount of refractive power, a bunch of correction lenses or their com-

binations are needed. Even worse is that it is a tiresome and time consuming procedure. Therefore many efforts have been made to develop an autorefractor. Among them two methods are worthwhile to be mentioned here. One is a scanning slit refractometer, and the other is based on a ray tracing (or optical path deviation) method.

2.1 Scanning slit refractometer based on retinoscopy

A scanning slit refractometer uses the same principle and scheme as the retinoscope. The main difference is that the eye of the examiner is replaced with an objective lens, a slit and two photodiodes. To enhance the measurement speed, a rotating slit wheel is used for the test light, as shown in Fig. 5 [1,22].

The objective lens is adjusted to have the conjugate image of the photodiodes be located onto the surface (or pupil) of the patient's eyeball. The patient is asked to see a fixation target for relaxation of accommodation. Then the scheme becomes exactly the same as the case of the retinoscope. However, since the motion of the test light is controlled with the rotating slit wheel and the motion of the reflected light is measured with the two photodiodes located at the examiner's retina position of the retinoscope case, the myopia or hyperopia can be automatically identified.

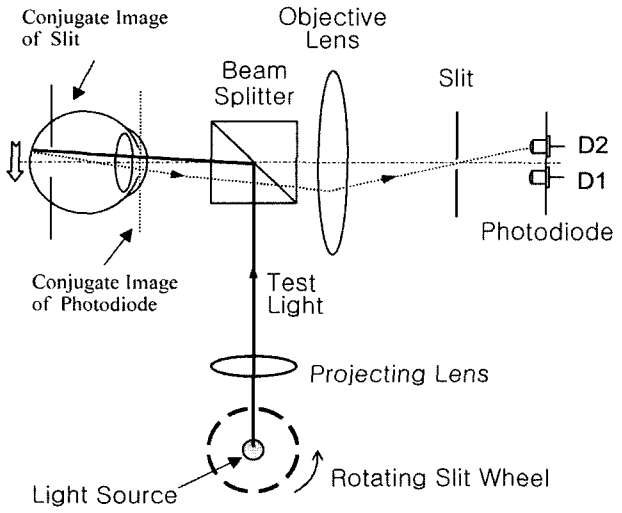

FIG. 5. A schematic diagram of a scanning slit refractometer based on retinoscopy.

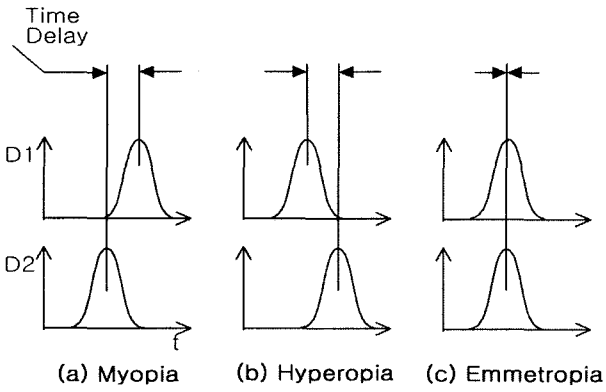

FIG. 6. The typical time delay between D1 and D2 signals with respect to the refractive condition of an eye.

For the myopia, the reflected light is in the 'against motion' with respect to the test light scanned by the rotating slit wheel. Fig. 5 shows that when the test light is reflected at the upper part of the retina of a myopic eye, the upper photodiode D2 is activated earlier than the lower photodiode D1, as shown in Fig. 6(a). For the hyperopia, due to the 'with motion', the reverse thing happens so that D2 is activated later against D1 as shown in Fig. 6(b). For the emmetropia case, due to the 'neutral motion', both photodiodes are activated at the same time without any time delay as shown in Fig. 6(c). The amount of the time delay between the photodiodes can be used to get the refractive power of the patient.

Astigmatism can be also measured with the same scheme as the retinoscope by simply adding rotation of the test light across the azimuthal angle of the patient eye. This measurement scheme is used in the refractometer of Nidek and the modified refractometer of Topcon.

2.2 Autorefractor based on ray tracing

The refractive power of an eye can be measured by tracing the light ray coming from a point on the patient's retina. Fig. 7 gives the schematic of the autorefractor based on ray tracing [23]. At first, the beam coming from a LED light source is focused on the retina of a patient by adjusting the projecting lens.

The combination of the objective and the detector lenses makes the aperture be conjugated with the pupil

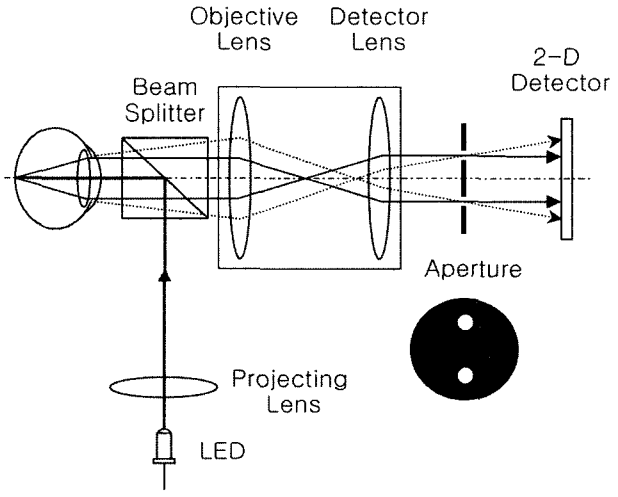

FIG. 7. A schematic diagram of an autorefractor based on ray tracing.

of a patient. The aperture has two pin-holes in a separated distance. Finally a 2-D detector, such as a charge-coupled device, measures the beams coming out of the aperture. Each pin-hole gives one light spot on the detector. Then the relative position between the two light spots coming from the two pin-holes gives the refractive power of the patient.

The beam focused on the retina forms a secondary light source that illuminates the whole area of the eye from inside. After passing through the eye, the light becomes parallel when the eye is emmetropic, because the secondary light source is just at the focal point of the eye. Therefore the beam passes through the pin-holes at the aperture with the normal angle and gives two points at the detector. In this emmetropia case, the lateral locations of the light spots on the detector are the same as the ones of the pin-holes. The solid arrow lines of Fig. 7 indicate the trace of the ray for the emmetropia.

While, for the hyperopia, the light coming out of the eye is diverging since the secondary light source is inside the focal point of the eye. Therefore the light ray passes the pin-holes with a diverging angle as shown with the dashed lines in Fig. 7. It gives two points on the detector but the distance between them becomes large compared with the emmetropia case. For the myopia, the reverse thing happens. The beam is converging just after the eye and directed into the pin-holes with a converging angle due to the objective and detector lens combination. It gives two points also on the detector but the relative distance becomes small compared with the emmetropia.

From this principle, by measuring the locations of the two light spots on the 2-D detector, it is possible to get the spherical refractive power, the cylindrical refractive power and the angular orientation of the cylindrical refractive power. As discussed above, depending on the refractive power of the patient's eye, the light coming out of the eye is parallel for the emmetropia, converging for the myopia and diverging for the hyperopia.

The wavefront error at the pupil can be expressed with the optical path difference (*OPD*). The *OPD* is approximately given as a linear combination of the first three Zernike polynomials [12,24]:

$$OPD(x,y)=\alpha(2x^2+2y^2-1)+\beta(x^2-y^2)+\gamma(2xy). \quad (1)$$

In the mean time, the linear coefficients can be determined from the location of light spots on the 2-D detector. From the definition of the *OPD*, the partial derivative of the *OPD* gives the lateral deviation of the light spots on the detector plane [12];

$$\frac{\Delta X_i}{L}=\frac{\partial OPD(x,y)}{\partial x}\Big|_{x=x_i,y=y_i}, \quad (2)$$

$$\frac{\Delta Y_i}{L}=\frac{\partial OPD(x,y)}{\partial y}\Big|_{x=x_i,y=y_i}, \quad (3)$$

where L is the distance between the aperture and the 2-D detector. Fig. 8 shows that ΔX_i and ΔY_i are the deviation from the spot position, (x_i, y_i), of the emmetropia case for each pin-hole i (i = 1, 2). We can find the coefficients in Eq. (1) by solving Eqs. (2) and (3).

The linear coefficients α, β and γ are related with the spherical refractive power (S), the cylindrical refractive power (C), and the angular orientation of the cylindrical refractive power (Φ) of the eye in the conventional ophthalmic negative-cylinder form through [12,25]

$$C=-\frac{4}{R^2}\sqrt{\beta^2+\gamma^2}, \quad (4)$$

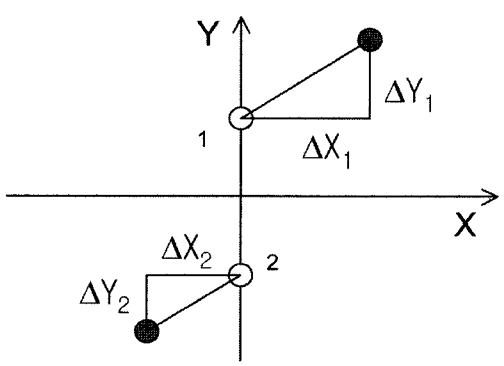

FIG. 8. Deviation of light spots on a CCD plane.

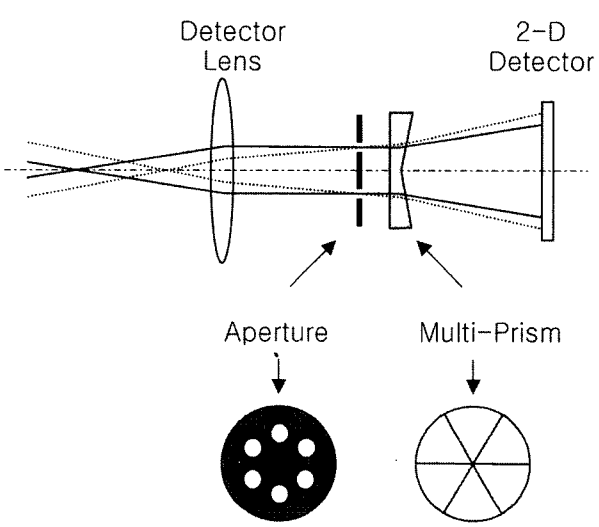

FIG. 9. This autorefractor uses the 6 pin-holes and the multi-prism in order to increase the measuring accuracy of the refractive power.

$$S = -\frac{4\alpha}{R^2} - \frac{C}{2}, \tag{5}$$

$$\Phi = \frac{1}{2}\tan^{-1}\left(\frac{\gamma}{\beta}\right), \tag{6}$$

where R is the pupil radius.

To increase the accuracy of the measurement, it is useful to increase the number of pin-holes at the aperture. Huvitz company, Korea, uses 6 pin-holes for its autorefractor as shown in Fig. 9. To enhance the *OPD* movement, a special multi-prim is utilized, which is composed of 6 conventional prisms. Each prism deviates the ray coming from the corresponding pin-hole outward of the detector center. This scheme also has the benefit of reducing the minimum pupil size necessary for measurements.

3. Wavefront analyzer

Even though the retinoscope and the autorefractor are powerful in measuring the visual acuity, they give only the value averaged over the whole area of the eye. Since a human eye can have a non-uniform refractive power across the area of the eye, it is necessary to measure the optical aberration of the eye at each individual point for more precise diagnosis. A wavefront analyzer has been developed for this purpose. Some of the most popular wavefront analyzers for eye diagnosis are a Tscherning aberroscope, a Shack-Hartmann wavefront analyzer, a scanning slit refractometer, a retinal ray tracing technology and a spatially resolved refractometer [13-18]. Among them, in this article, the principle of the scanning slit refractometer and the Tscherning's scheme are briefly introduced and the detail analysis on the Shack-Hartmann's scheme is presented.

3.1 Scanning slit refractometer for measuring the wavefront error

A scanning slit refractometer which was described in Section 2.1 can be improved to work as a wavefront analyzer by increasing the number of measuring points [2]. As shown in Fig. 10, both the photodetector (PD) and the scanning chopper wheel rotate around an optical axis synchronously to measure the refractive power at each 1-degree meridian. The 180 degrees rotation covers 360 degrees meridian of the eye by using the PD elements located in a symmetrical layout.

The 4 pairs of PD elements measure the lights at 4-diameters on the corneal plane, respectively. A pair of PD elements placed in a lateral direction are used to detect the center of the 4 pairs of PD elements. The time difference at any point on the cornea is generated based on the distance between the retina and the conjugate image of the aperture. The time differences between the center and each PD element are converted into the refractive power of the patient.

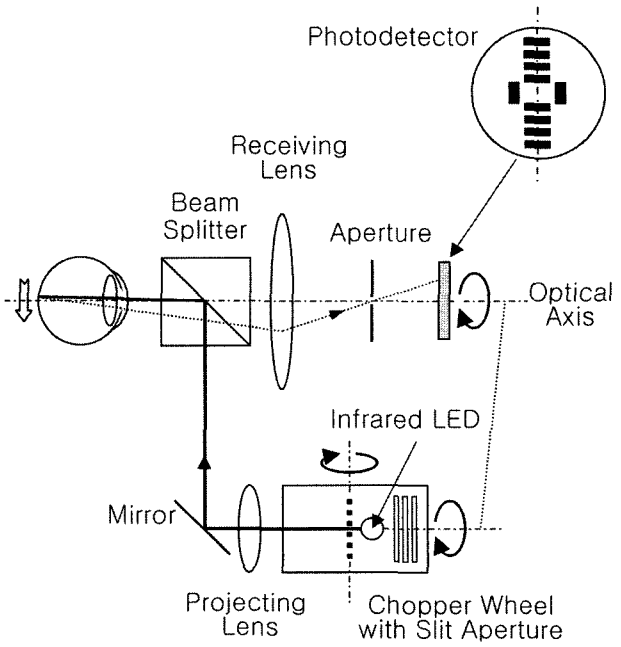

FIG. 10. A schematic diagram of a scanning slit refractometer for measuring the wavefront error.

3.2 Tscherning aberroscope

Tscherning proposed a method that could measure the aberration of a human eye in 1894 [6]. A patient was asked to see a distant light source such as a star through an optical lens of about +5 D with a grid at the lens surface and then asked to draw what he or she saw. The grid pattern was imaged on the retina, but each point of the image could be assumed to have passed through a different part of the eye. Therefore, the aberration of the eye affected the image of the pattern.

For the emmetropia, the image drawn by the patient was very similar to the grid pattern itself. However, for the ametropic eye, the drawn image became distorted. Its principle was very simple but it was a subjective method. The patient should be asked to draw what he or she saw. In 1997, the Dresden wavefront analyzer was developed at Technical University of Dresden, Germany. It was based on the same principle as the Tscherning's one but designed to operate in an objective mode [17,26].

The schematic of the Dresden wavefront analyzer is depicted in Fig. 11. A laser beam is collimated and directed on a mask having many small apertures in a pattern as shown in Fig. 11(a). This dot pattern is imaged by the aberroscope lens on the retina. Therefore the patient becomes able to see the dot pattern on the mask. When the patient's eye is in a normal state, the exactly identical pattern of the mask will be imaged on

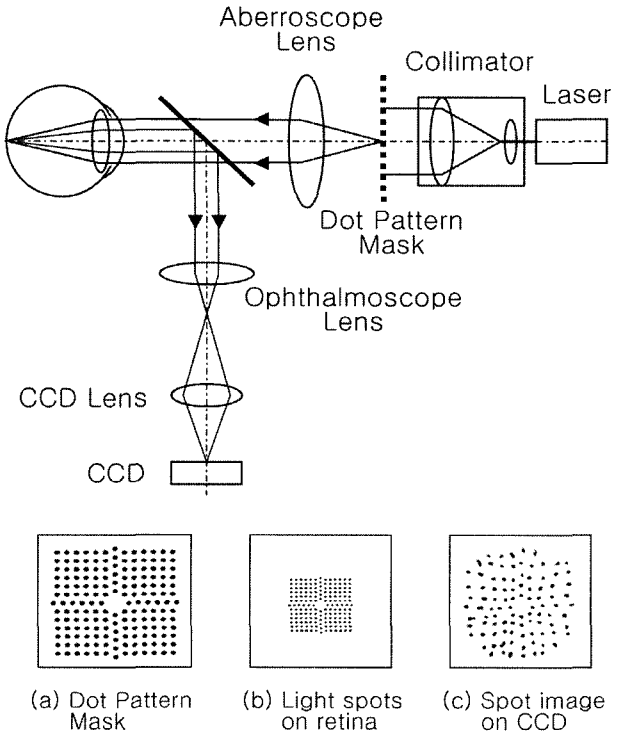

FIG. 11. A schematic diagram of a Tscherning aberroscope.

the retina as shown in Fig. 11(b). However, if there is the refractive error in the eye, then the imaged pattern becomes distorted.

In the old Tscherning's scheme, the pattern imaged on the retina was drawn by the patient, however, in this new scheme, the image on the retina is optically extracted and recorded by a CCD (charge-coupled device) without the help from the patient. The combination of the ophthalmoscope lens and the CCD lens images the retina of the patient on the CCD plane. Fig. 11(c) shows one of the examples recoded by the CCD. We can see that the pattern on the CCD is highly distorted. Therefore, by analyzing the spot image on the CCD, the aberration of the patient eye can be obtained. In general, the method of comparing the CCD image of the patient with the one resulted from an ideal model eye is used.

Since at the very center of the cornea of the patient eye, there is appreciable amount of unwanted reflection, which is directed into the CCD and reduces the image quality. Therefore, to reduce the effect of the unwanted reflection, the beam impinging at the very center of the cornea is blocked. The missing apertures at the very center of the mask, as can be seen in Fig. 11(a), are made for this purpose.

3.3 Shack-Hartmann wavefront analyzer

The first concept of the Shack-Hartmann wavefront analyzer was proposed by Smirnov in 1961 [27]. The basic structure which used a Hartmann screen [28] was

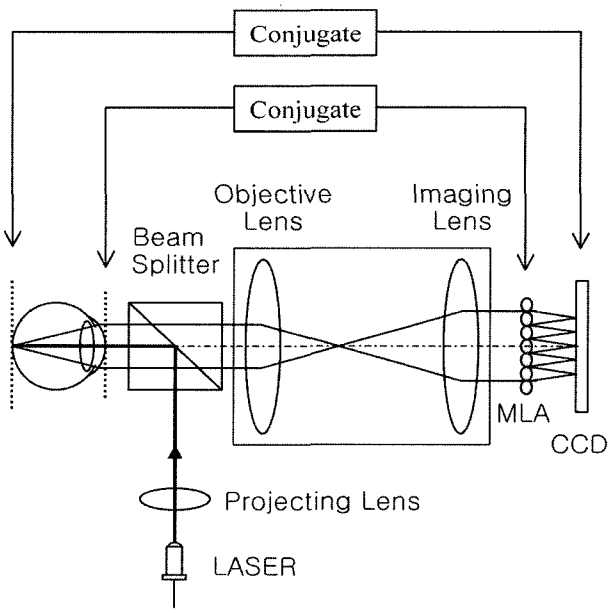

FIG. 12. A schematic diagram of a Shack-Hartmann wavefront analyzer.

completed by Shack in 1971 [29]. The first clinical test was reported by Liang in 1994 [12]. Currently, it is widely adapted as the very essential diagnostic instrument for the corneal ablation (or refractive surgery) field. The Shack-Hartmann wavefront analyzer [15] is very powerful in measuring the distribution of the refractive power across the whole pupil area of a patient.

The operation scheme is depicted in Fig. 12. At first, the beam coming from a laser source is directed into the eyeball and focused on the retina of the patient by adjusting the projecting lens. The focused beam forms a secondary point light source on the retina and emerged as a plane wave for the normal eye case. If the eye has a problem in its refractive power or power distribution, the wavefront of the emerging beam is distorted. This distortion is detected by the CCD with the help of the relay lens and the micro-lens array (MLA) in the figure.

The relay lens, composed of an objective lens and an imaging lens, conjugates the pupil plane with the MLA plane. Therefore, the wavefront of the beam at the pupil plane is duplicated at the MLA plane. Since the MLA is composed of many micro-lenses, it gives many spots on the CCD plane. The CCD is located at the focal plane of the MLA. According to the shape of the wavefront, the spots imaged on the CCD have different configurations.

When the eye is normal, the CCD image follows the configuration of the micro-lenses of the MLA. However, when the eye has a problem, the CCD image is distorted from the micro-lens configuration. Actually, the inclining angle of the wavefront affects the position of the spot image on the CCD. Thus, by analyzing the

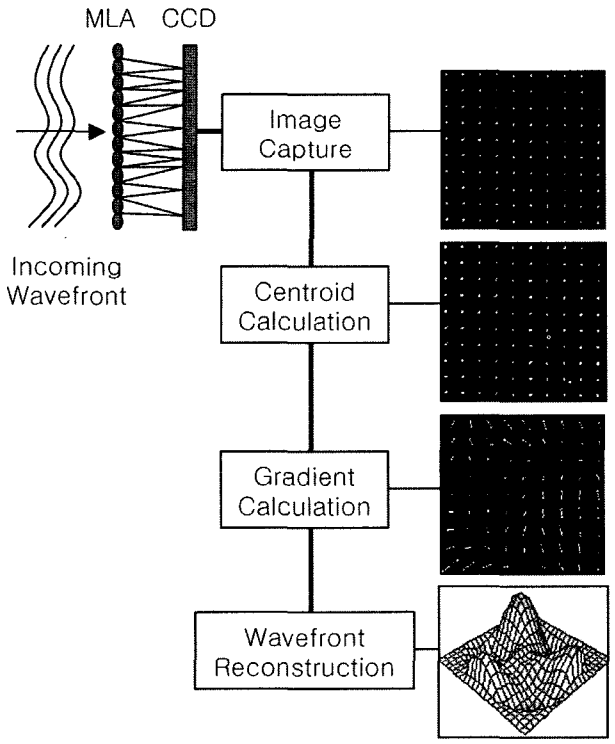

FIG. 13. The procedure of reconstructing the wavefront.

CCD image, it is possible to get the information about the wavefront aberration. Finally, from this measured wavefront aberration information, the wavefront at the pupil can be reconstructed [12,30-31].

Fig. 13 shows the procedure of reconstructing the wavefront from the CCD image. If the eye is in a normal state, the array of light spots in the CCD image will be in a regular pattern. However, due to the aberration, the light spots will be deviated. Therefore, it is necessary to find the ideal site of each light spot, which is made in the centroid calculation process. The centroid calculation gives the position of each spot for the ideal normal eye. Therefore this process should be very precise. By comparing the captured image with the ideal image, the gradient of the deviation is calculated. From this information, the wavefront of the patient eye is reconstructed with some mathematical manipulation.

The wavefront error of the patient eye is defined as the optical path difference between the wavefront of the patient and the one of an ideal eye. In general, the wavefront error is a function of the pupil coordinate but also of the MLA coordinate due to the relay lens. The wavefront error function $W(x, y)$ can be expanded with the Zernike polynomials $Z_k(x, y)$ as [12,24,30]

$$W(x,y)=\sum_{k=1}^{\infty}\alpha_k Z_k(x,y) \quad (7)$$

The Zernike polynomials are orthogonal to each other over the unit circle [24] and the coefficient α_k is directly related with particular aberration of the eye. It can be approximately presented with a finite number of polynomials;

$$W(x,y)=\sum_{k=1}^{n}\alpha_k Z_k(x,y) \quad (8)$$

where n is the number of Zernike polynomials involved in calculation.

The deviation, $(\triangle X_i, \triangle Y_i)$, of the light spot resulted by the i-th micro-lens from its ideal position is measured by the CCD and given by the partial derivatives of the wavefront error function in Eq. (8) as

$$\Delta X_i = F\frac{\partial W(x,y)}{\partial x}\Big|_{x=x_i,y=y_i}, \quad (9a)$$

$$\Delta Y_i = F\frac{\partial W(x,y)}{\partial y}\Big|_{x=x_i,y=y_i}, \quad (9b)$$

where, the constant F is the focal length of a MLA. Inserting Eq. (8) into Eq. (9) gives

$$\Delta X_i = F\sum_{k=1}^{n}\alpha_k\frac{\partial Z_k}{\partial x}\Big|_{x=x_i,y=y_i}, \quad (10a)$$

$$\Delta Y_i = F\sum_{k=1}^{n}\alpha_k\frac{\partial Z_k}{\partial y}\Big|_{x=x_i,y=y_i}. \quad (10b)$$

By using new constants defined as

$$A_{i,k}\equiv\frac{\partial Z_k}{\partial x}\Big|_{x=x_i,y=y_i}, \quad (11a)$$

$$A_{m+i,k}\equiv\frac{\partial Z_k}{\partial y}\Big|_{x=x_i,y=y_i}, \quad (11b)$$

we have Eqs. (10) and (11) as a vector product form of

$$P_i\equiv\frac{\Delta X_i}{F}=\sum_{k=1}^{n}A_{i,k}\alpha_k, \quad (12a)$$

$$P_{m+i}\equiv\frac{\Delta Y_i}{F}=\sum_{k=1}^{n}A_{m+i,k}\alpha_k, \quad (12b)$$

where m is the number of light spots involved in calculation. It is exactly the same as the matrix equation in a form of

$$\begin{bmatrix}P_1\\ \vdots\\ P_{2m}\end{bmatrix}=\begin{bmatrix}A_{1,1} & \cdots & A_{1,n}\\ \vdots & & \vdots\\ A_{2m,1} & \cdots & A_{2m,n}\end{bmatrix}\begin{bmatrix}\alpha_1\\ \vdots\\ \alpha_n\end{bmatrix}. \quad (13)$$

However the matrix $[A]$ in the middle of the Eq. (13)

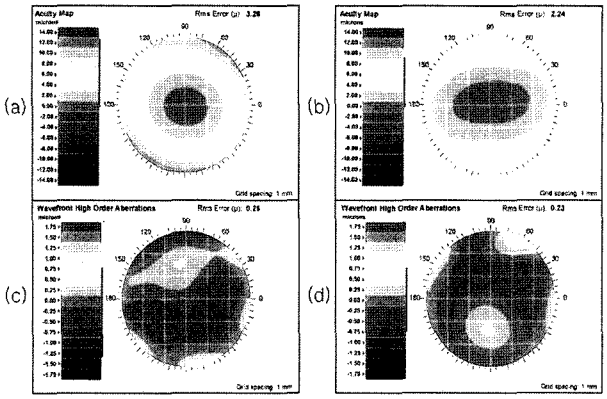

FIG. 14. An example of the results measured by a Shack-Hartmann wavefront analyzer.

is not square in general. Therefore a least square solution instead of the exact solution is expected. By using a pseudo inverse of the matrix, we have the coefficient vector $[\alpha]$ as the function of the measurable deviation vector $[P]$;

$$[\alpha] = [A^T A]^{-1}[A^T][P] \tag{14}$$

From the calculated linear coefficients of Zernike polynomials, the aberration of the patient eye is analyzed.

Fig. 14 shows an example of the measuring results made with the Shack-Hartmann wavefront analyzer (VISX, WaveScan). The first two inset figures, (a) and (b), are called acuity maps of the left eye and the right eye of a patient, respectively. They are related to the lower order aberration of the eyes. From the figures, we can say that the left eye has a -2.05 D spherical vertex power, -0.90 D cylindrical vertex power, and 168 degree of cylinder axis. While the right eye has -0.61 D spherical vertex power, -1.68 D cylindrical vertex power, and 4 degree cylinder axis. Both eyes of the patient can be said having rather severe asymmetricity in their refractive powers. The inset figures, (c) and (d), show the higher order aberration of the left and right eyes, respectively. As a factor of wavefront aberration, the RMS (root mean square) error of the left eye is measured as 0.25 ㎛, which is a little bit higher than that of the right eye, 0.23 ㎛. Such higher order aberration may cause glaring in a night vision but can not be corrected with conventional eye glasses, unfortunately.

III. DISCUSSION AND SOME TECHNICAL ISSUES

It is commonly accepted that the number of glasses-wearers has been increased with civilization. There might be many factors that hurt the health of a human eye. Finding the factors and preventing the degradation of the eye are the best approach, however, we do not have an effective solution owing to the complexity and multitude of the causes of defective vision. Correcting the vision with eye glasses is used as the best remedy. Therefore, analyzing and measuring the visual acuity and the refractive error of an eye becomes more important. The refractometer is a prominent instrument which has been developed for this purpose.

The human eye is designed to operate mainly in the visible wavelength range. The transmittance into the eyeball, through the cornea, is high at both the visible and near IR regions. However the reflectance at the fundus of an eye is larger in the IR region [20,32]. Generally, the refractometer uses the light reflected at the fundus as a secondary light source. Therefore, IR sources are the most suitable for the refractometers. They effectively examine the patient without causing discomfort since the patient cannot visually recognize the IR radiation. Fortunately, many low-cost light sources based on semiconductor materials are available.

There are some technical problems to be overcome in development of a refractometer. The relaxation of accommodation of the patient is important for the accurate measurement with a refractometer. To lead the relaxation of a patient's accommodation, a fogging method is used, where the fixation target of a scenery picture (or a geometrical pattern) is intentionally fogged. However, in general, it is not easy to get the complete relaxation of accommodation.

The optical system that gives a good linearity with the refractive power of the eye is one of the big issues that are waiting development. On the other hand the high reflection of the beam incident right on the center of the cornea causes difficulties in designing the optical system. The reflectance and scattering at each surface of the optic system, including the eye itself, degrades the performance of the instrument. Thus a means of reducing or avoiding the effect of unwanted stray light is necessary.

The spot size of the secondary light source generated at a point on the fundus of the eye affects the accuracy of the instrument. For the wavefront analyzer case, the smaller spot size allows more precise centroid estimation. For a normal eye, a collimated beam is focused into a small spot on the fundus by the lens of the eye. However, when the eye has a problem in its refractive power, it is not a small spot anymore. Therefore, adjustment in the optical projecting system is necessary. According to the refractive power of the patient eye, the diverging angle of the input beam should be adjusted optically. Considering that a usual refractometer has a measurement dynamic range of -20 D ~ +20 D, an intensive effort is asked in its optical and electronic control systems.

Speckle is another factor that degrades the performance.

In general, the speckle phenomenon becomes less important by using a high incoherent light source such as a white light. However, the size of the secondary light source becomes smaller when a coherent light source such as a laser is used. As a compromise, a SLD (superluminescent diode) is used. It has a rather wide wavelength spectrum but can be easily focused.

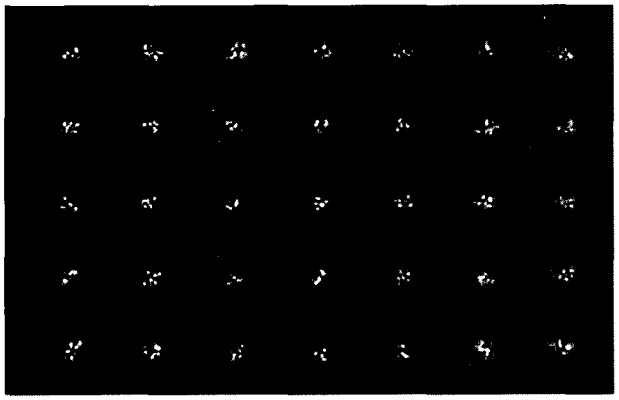

FIG. 15. Speckle noise of the light spots.

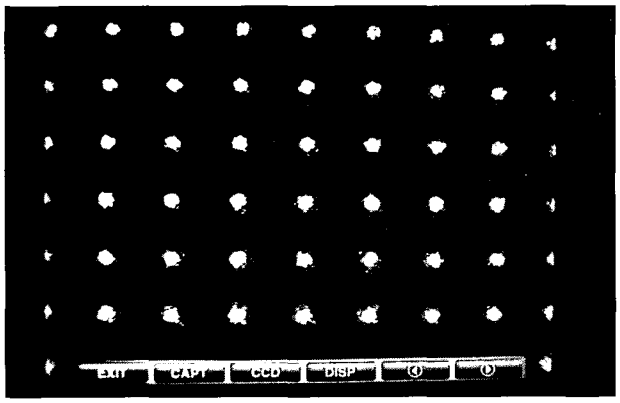

(a)

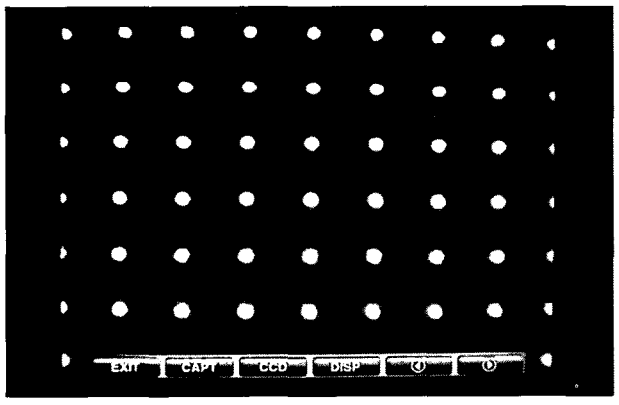

(b)

FIG. 16. Light spots imaged on CCD. The images were taken (a) without, and (b) with rotating the hologram diffuser, respectively.

In our laboratory, a Shack-Hartmann wavefront analyzer was implemented and the measurements were made with different light sources for a normal model eye. Fig. 15 shows the speckle patterns which has been obtained with a typical IR diode laser as a light source. Even though a SLD was used in our laboratory, the speckle was not reduced sufficiently. The speckle may be reduced by using a rotating aperture [33] or a rotating diffuser.

With a SLD (Hamamatsu model L-8414-41; center wavelength 830 nm and spectral bandwidth 15 nm), the same experiment was made but with inserting a hologram diffuser (diffusing angle: 0.5 deg., Luminit Co.). A hologram diffuser was inserted just in front of the SLD and rotated with a speed of about 8000 RPM (revolutions per minute). As shown in Fig. 16(b), the CCD image became very clear without appreciable speckle noise. For comparison, the image taken without rotating the diffuser is shown in Fig. 16(a).

Other factors degrading the performance of the refractometer are the image sensor noise, the limited size of the image sensor, the magnitude and profile of spot irradiance distribution, and so on [34-35]. The centroid estimation for the wavefront analyzer is very essential to the performance. Even though there have been many efforts, still it needs improvement. Currently, center of gravity and correlation algorithm methods are used [36-37], but they are still far from satisfactory.

Zernike polynomials basically form a very suitable function set describing the refractive power distribution of a human eye. They are orthogonal to each other over the unit circle and lower order ones are directly related with the lens aberration. However, since the polynomials are based on a polar coordinate, when the corneal apex is off centered from the pupil, careful correction should be made. Furthermore, it is impossible to describe a partially inclined plane with a finite number of Zernike polynomials.

IV. SUMMARY

Even though a human eye is composed of a simple lens, it is a high precision optical system. An ideal eye is aberration-free and adaptive with its ability to adjust the focal length automatically. However these days many people are suffering from poor vision due to imperfect eye. The accurate measurement of the refractive power of a human eye is becoming important with increasing number of patients who need the correcting glasses or the refractive surgery. In this article we have briefly reviewed the development history of refractometers. The optical systems and the underlining measurement principles governing the operation of various types of refractometers also have been discussed. The development of refractometer

enables more precise and accurate measurement of refractive power by itself. In addition to this, it will allow ophthalmologists to obtain valuable informations for diagnosis, and also researchers to expand the horizon of their fields related with optesthesia. Finally, some technical issues and problems that need to be overcome for getting better performance have been discussed.

ACKNOWLEDGMENT

This research was supported in part by the Advanced Technology Center (ATC) project of Ministry of Commerce Industry and Energy (MOCIE) and by the Korea-China Joint Research Project of Ministry of Science and Technology (MOST).

*Corresponding Author: dsko@mokwon.ac.kr

REFERENCES

[1] T. Hellmuth, "Sensors in Ophthalmology," *Sensors Update*, vol. 3, no. 1, pp. 289-323, 2001.

[2] S. M. MacRae, R. R. Krueger, and R. A. Applegate, *Customized corneal ablation* (Slack, Thorofare, 2001).

[3] H. C. Howland, "The history and methods of ophthalmic wavefront sensing," *J. Refract. Surg.*, vol. 16, no. 5, pp. S552-S553, 2000.

[4] L. N. Thibos, "Principles of Hartmann-Shack aberrometry," *J. Refract. Surg.*, vol. 16, no. 5, pp. S563-S565, 2000.

[5] S. Buck, *Der geschärfte blick zur geschichte der brille und ihrer verwendung in Deutschland seit 1850*, Ph.D. Thesis, Philipps Univ., Germany, 2002.

[6] M. Tscherning, "Die monochromatischen aberrationen des menschlichen auges," *Z. Psychol. Physiol. Sinn.*, vol. 6, pp. 456-471, 1894.

[7] B. Howland and H. C. Howland, "Subjective measurement of high-order aberrations of the eye," *Science*, vol. 193, pp. 580-582, 1976.

[8] H. C. Howland and B. Howland, "A subjective method for the measurement of monochromatic aberrations of the eye," *J. Opt. Soc. Am.*, vol. 67, no. 11, pp. 1508-1518, 1977.

[9] R. E. Reason, "Sight-testing apparatus", US patent 2049222, 1936.

[10] G. Collins, "The electronic refractometer," *Br. J. Physiol. Opt.*, vol. 1, pp. 30-40, 1937.

[11] N. Roth, "Automatic optometer for use with the undrugged human eye," *Rev. Sci. Instrum.*, vol. 36, no. 11 pp. 1636-1641, 1965.

[12] J. Liang, B. Grimm, S. Goelz, and J. F. Bille, "Objective measurement of wave aberrations of the human eye with the use of a Hartmann-Shack wave-front sensor," *J. Opt. Soc. Am. A*, vol. 11, no. 7, pp. 1949-1957, 1994.

[13] E. Moreno-Barriuso, S. Marcos, R. Navarro, and S. A. Burns, "Comparing laser ray tracing, the spatially resolved refractometer, and the Hartmann-Shack sensor to measure the ocular wave aberration," *Optom. Vis. Sci.*, vol. 78, no. 3, pp. 152-156, 2001.

[14] E. Moreno-Barriuso and R. Navarro, "Laser ray tracing versus Hartmann-Shack sensor for measuring optical aberrations in the human eye," *J. Opt. Soc. Am. A*, vol. 17, no. 6, pp. 974-985, 2000.

[15] B. C. Platt and R. Shack, "History and principles of Shack-Hartmann wavefront sensing," *J. Refract. Surg.*, vol. 17, no. 5, pp. S573-S577, 2001.

[16] S. A. Burns, "The spatially resolved refractometer," *J. Refract. Surg.*, vol. 16, no. 5, pp. S566-S569, 2000.

[17] M. Mrochen, M. Kaemmerer, P. Mierdel, H.-E. Krinke, and T. Seiler, "Principles of Tscherning aberrometry," *J. Refract. Surg.*, vol. 16, no. 5, pp. S570-S571, 2000.

[18] V. V. Molebny, S. I. Panagopoulou, S. V. Molebny, Y. S. Wakil, and I. G. Pallikaris, "Principles of ray tracing aberrometry," *J. Refract. Surg.*, vol. 16, no. 5, pp. S572-S575, 2000.

[19] B. J. Wilson, K. E. Decker, and A. Roorda, "Monochromatic aberrations provide an odd-error cue to focus direction," *J. Opt. Soc. Am. A*, vol. 19, no. 5, pp. 833-839, 2002.

[20] W. N. Charman, *Handbook of Optics*, vol. 1, 2nd ed., M. Bass, E. W. Van Stryland, D. R. Williams, and W. L. Wolfe eds. (McGraw-Hill, New York, 1995), chap. 24.

[21] *Ophthalmic Test*, The Korean Ophthalmological Society ed. (Jin Publishing, Seoul, 2002).

[22] M. Nohda, I. Umemura, and T. Arai, "Eye-refractometer device", US patent 4390255, 1983.

[23] K. Sekiguchi, "Ophthalmic measuring apparatus", US patent 4878750, 1989.

[24] R. J. Noll, "Zernike polynomials and atmospheric turbulence," *J. Opt. Soc. Am.*, vol. 66, no. 3, pp. 207-211, 1976.

[25] T. O. Salmon, R. W. West, W. Gasser, and T. Kenmore, "Measurement of refractive errors in young myopes using the COAS Shack-Hartmann aberrometer," *Optom. Vis. Sci.*, vol. 80, no. 1, pp. 6-14, 2003.

[26] R. P. Mierdel, H. E. Krinke, W. Wiegand, M. Kaemmerer, and T. Seiler, "Messplatz zur bestimmung der monochromatischen aberration des menschlichen auges," *Ophthalmologe,* vol. 96, pp. 441-445, 1997.

[27] M. S. Smirnov, "Measurement of the wave aberration of the human eye," *Biofizika*, vol. 6, pp. 687-703, 1961.

[28] J. Hartmann, "Bemerkungen uber den Bau und die Justirung von Spektrographen," *Z. Instrumentenkd.*, vol. 20, pp. 47-58, 1900.

[29] R. V. Shack and B. C. Platt, "Production and use of a lenticular Hartmann screen," *J. Opt. Soc. Am.*, vol. 61, p. 656, 1971.

[30] D. M. Topa, "Wavefront reconstruction for the Shack-Hartmann wavefront sensor," *Proc. SPIE,* vol. 4769, pp. 101-115, 2002.

[31] L. A. Poyneer, "Advanced techniques for Fourier transform wavefront reconstruction," *Proc. SPIE*, vol. 4839, pp. 1023-1034, 2003.

[32] W. J. Geeraets and E. R. Berry, "Ocular spectral characteristics as related to hazards from lasers and other light sources," *Am. J. Ophthalmol.*, vol. 66, no. 1, pp. 15-20, 1968.

[33] Y. Kawagoe, N. Takai, and T. Asakura, "Speckle reduction by a rotating aperture at the fourier transform plane," *Opt. Laser Eng.*, vol. 3, pp. 197-218, 1982.

[34] D. R. Neal, J. Copland, and D. A. Neal, "Shack-Hartmann wavefront sensor precision and accuracy," *Proc. SPIE*, vol. 4779, pp. 148-160, 2002.

[35] W. Jiang, H. Xian, and F. Shen, "Detection error of Shack-Hartmann wavefront sensors," *Proc. SPIE*, vol. 3126, pp. 534-544, 1997.

[36] S. Thomas, "Optimized centroid computing in a Shack-Hartmann sensor," *Proc. SPIE*, vol. 5490, pp. 1238-1246, 2004.

[37] L. A. Poyneer, *Correlation wave-front sensing algorithms for Shack-Hartmann-based adaptive optics using a point source*, Report No. UCRL-JC-152975, Lawrence Livermore National Lab. (Livermore, CA, USA), 2003.